OPTOELECTRONICS AND ADVANCED MATERIALS – RAPID COMMUNICATIONS Vol. 4, No. 8, August 2010, p. 1144 - 1148

Optimization of process conditions of textured gallium-doped zinc oxide films for thin film silicon solar cells

Q. QIAO, S. Z. WANG[a], K. Ma[b], Y. Q. WANG[b], G. C. ZHANG[b], Z. R. SHI[b], G. H. LI[a*]
School of Communication and Control Engineering, Jiangnan University, Wuxi 214122, China
[a]School of Science, Jiangnan University, Wuxi 214122, China
[b]Suntech Power Holdings Co., Ltd., Wuxi 214028, China

Textured gallium-doped zinc oxide (GZO) films were prepared by post etching sputter-deposited GZO films. In order to achieve balanced optical and electrical properties, GZO films were deposited at low temperature from targets with different gallium concentrations. With the purpose of extending etching time, buffer solutions such as acetic acid and sodium acetate were added to the traditional etchant 0.5 % HCl. Finally, the optimized textured GZO films were applied as front contacts in amorphous silicon solar cells. A short-circuit current density of 14.340 mA/cm^2 and an initial aperture area efficiency of 8.784 % were obtained on 16×16 cm^2 substrate.

(Received March 01, 2010; accepted August 12, 2010)

Keywords: Gallium-doped zinc oxide, Sputtering, Etching, Solar cells

1. Introduction

For thin film silicon solar cells, one of the most effective ways to increase conversion efficiency as well as decrease production cost is the improvement in the properties of the transparent conductive oxide (TCO) glass, which is commonly used as a front contact and an optical window in the p-i-n (superstrate) structure. The traditional commercial TCO glass, with its TCO layer consisting of SnO_2:F, is provided by only few manufacturers. The high price of SnO_2:F coated TCO glass takes up nearly 20% of the total cost of the thin film silicon solar cells. Nevertheless, SnO_2:F is not the best material for TCO glass, since the strong hydrogen plasma which is needed for fabricating high conductive p-type a-Si:H layer on SnO_2:F layer, will deoxidize and darken the SnO_2:F film, thus deteriorate the performance of the cell [1].

ZnO is thought to be one of the appropriate substitutes of SnO_2:F and solutions of such problems mentioned above. Generally, there are two approaches to fabricate textured ZnO films. One is to deposit textured ZnO:B films directly by LP-MOCVD, which suffer from poor thermal stability [2]. The other is to texture the sputter deposited doped ZnO films by post-deposition chemical etching. The most widely used dopant is aluminum, whose high reactivity would result in oxidation during the growth of AZO films. In contrast, gallium is more resistant to oxidation, leading to higher carrier concentration. In addition, the similarities in the radiuses of gallium (0.126 nm) and zinc (0.135 nm) and in the covalent bonds lengths of Ga-O (0.192 nm) and Zn-O (0.197 nm) would minimize the deformation of the ZnO lattice even in the case of high gallium concentration [3].

In this work, we focus on the optimization of process conditions of textured GZO films. Many previous studies showed an improvement in crystallinity of the AZO films when deposited at elevated temperature up to about 350 °C [4-6]. From the view of saving thermal budget and the possible application in flexible polymer substrates, however, high quality ZnO films should also be obtained in low temperature process. Based on this consideration, we study the influence of the target gallium concentration on the optical and electrical properties of GZO films deposited at relatively low temperature. With the aim of making the wet-chemical etching time long enough to be controllable in industrial processes, we improve the etchant solutions. Then, we investigate surface morphologies, haze spectra and structure properties of the textured films, respectively. Finally, we present the results on amorphous silicon solar cells fabricated on commercial SnO_2:F with standard p-i-n structure and on optimized textured GZO without and with p-type μc-Si:H layer inserted between GZO and p-type a-SiC:H layer.

2. Experimental

GZO films were prepared on float glass at 70 °C by rf-magnetron sputtering from ceramic GZO targets with 0.5, 2.5 and 3.2 wt.% of Ga_2O_3, respectively. The initial flat films were textured by wet-chemical etching. We

added acetic acid and sodium acetate, which were served as buffer solutions, to the traditional etchant 0.5 % HCl. The etching time was prolonged up to 120 s while maintaining good optical and electrical properties of the films. The thickness of deposited film was measured by surface profiler (P-16+, KLA Tencor), the sheet resistance was determined by a four-point-probe (DJ-II, Guangzhou Institute of Semiconductor), the surface morphology of the film was examined by atomic force microscope (XE-100, Park Systems), the orientation of the crystallites was investigated by X-ray diffraction (X'Pert PRO, Panalytical), the optical transmittance and haze factor of the film were measured by UV-Vis-NIR spectrophotometer (Cary 5000, Varian) and hazemeter (MFS-530, Hongming technology), respectively. Finally, a-Si:H p-i-n solar cells were fabricated by rf-PECVD on 16×16 cm^2 substrate of commercial SnO_2:F and optimized textured GZO, respectively. The J-V characteristics of the solar cells were investigated under standard test conditions (AM 1.5, 100 mW/cm^2 at 25 °C) using a sun simulator (93194A-1000, Newport).

3. Results and discussion

3.1 Influence of the target gallium concentration

For the application in thin film silicon solar cells, especially for μc-Si:H based solar cells, TCO has to combine low resistivity and high transparency in the visible and near infrared (NIR) spectral range. High carrier concentration leads to low resistivity but high free carrier absorption loss in the long wavelength region. There exists a tradeoff between the low resistivity and low free carrier absorption loss. In previous studies, Agashe et al. and Berginski et al. investigated the influence of the target alumina concentration on the optical and electrical properties of AZO films, respectively [6,7]. In this work, under the same sputter parameters, we deposited GZO films from ceramic targets with 0.5, 2.5 and 3.2 wt.% of Ga_2O_3, respectively. Fig. 1 shows the optical transmittance in the range of 400-1200nm. Comparing the textured and flat GZO films, the increased scattering reduces the coherent part of the light, and results in smoothing interference fringes of the transmittance curves. According to the Burstein-Moss effect, the short wavelength turn-on edge is shifted to smaller wavelengths with increasing of target gallium concentration [8,9]. The average transmittance in the visible range is similar for different target gallium concentrations, while in the red and NIR range, the difference in transmittance between the high and low target gallium concentration is more pronounced. On the other hand, as the increase of the target gallium concentration, the number of free carriers in deposited GZO films increases and the value of sheet resistance decreases. Figure of merit, F_{TC}, is introduced to compare the balanced optical and electrical performances [10].

$$F_{TC} = \frac{T_{lum}^{10}}{R_{sheet}} \qquad (1)$$

$$T_{lum} = \frac{\int f(\lambda)T(\lambda)d\lambda}{\int f(\lambda)d\lambda} \qquad (2)$$

where T_{lum}, R_{sheet}, f(λ) and T(λ) are transmittance, sheet resistance, solar spectral irradiance and measured transmittance, respectively. Larger value of F_{TC} means better balanced optical and electrical properties. From Table 1, the optimum values of F_{TC} occur at the target gallium concentration of 3.2 and 0.5 wt.% for the spectral range of 400-800 nm and 400-1200 nm, respectively.

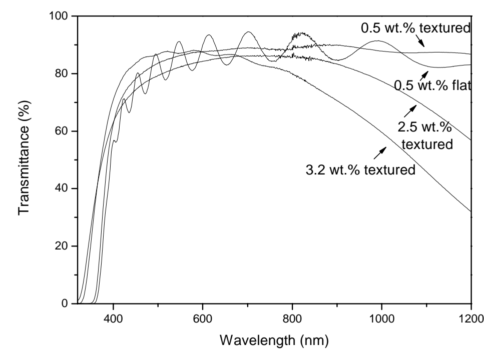

Fig. 1. Optical transmission of textured and flat GZO films.

Table 1. Optical and electrical parameters for various target gallium concentrations (λ_1 stands for 400-800 nm, λ_2 stands for 400-1200 nm).

	3.2 wt.%		2.5 wt.%		0.5 wt.%	
	λ_1	λ_2	λ_1	λ_2	λ_1	λ_2
R_{sheet} (Ω/sq)	5.7		10.7		14.5	
T_{lum} (%)	85.1	78.3	82.3	81.0	85.5	86.5
F_{TC} (10^{-2} Ω^{-1})	3.49	1.52	1.32	1.14	1.44	1.61

3.2 Optimization of the etching process

For smooth GZO films, the etching process usually adopted is a short dip in 0.5 % HCl, and the etching time is typically around 15 s [11], which is too short to be controllable in industrial processes. Moreover, Kluth et al. showed that the etching rate increased with decreasing substrate temperature due to low compactness of deposited AZO films [12]. For the etching of GZO films deposited at low temperature, we added buffer solutions, such as acetic acid and sodium acetate, so that the pH changed less than

what it would be if 0.5 % HCl was not buffered.

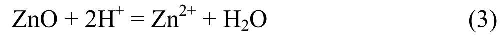

$$ZnO + 2H^{+} = Zn^{2+} + H_2O \quad (3)$$

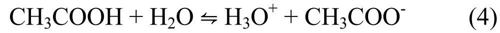

$$CH_3COOH + H_2O \leftrightharpoons H_3O^{+} + CH_3COO^{-} \quad (4)$$

Following Le Chatelier's principle, when hydrogen ions (H^+) are added to the buffer solution, CH_3COOH would be formed first, as there are H^+ on the right-hand of the equilibrium (4). Oxygen site in the ZnO structure would not be attacked immediately. Therefore, etching time can be extended. As observed from Fig. 2, the flat GZO films are anisotropically etched leading to a crater-like texture surface, whose root mean square roughness (δ_{rms}) values are 46.919 nm and 72.929 nm as determined by AFM, for etching time of 60 s and 90 s, respectively.

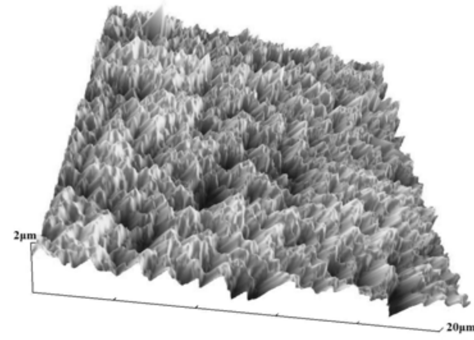

Fig. 2. AFM micrograph of a textured GZO film with δ_{rms} of 72.929 nm.

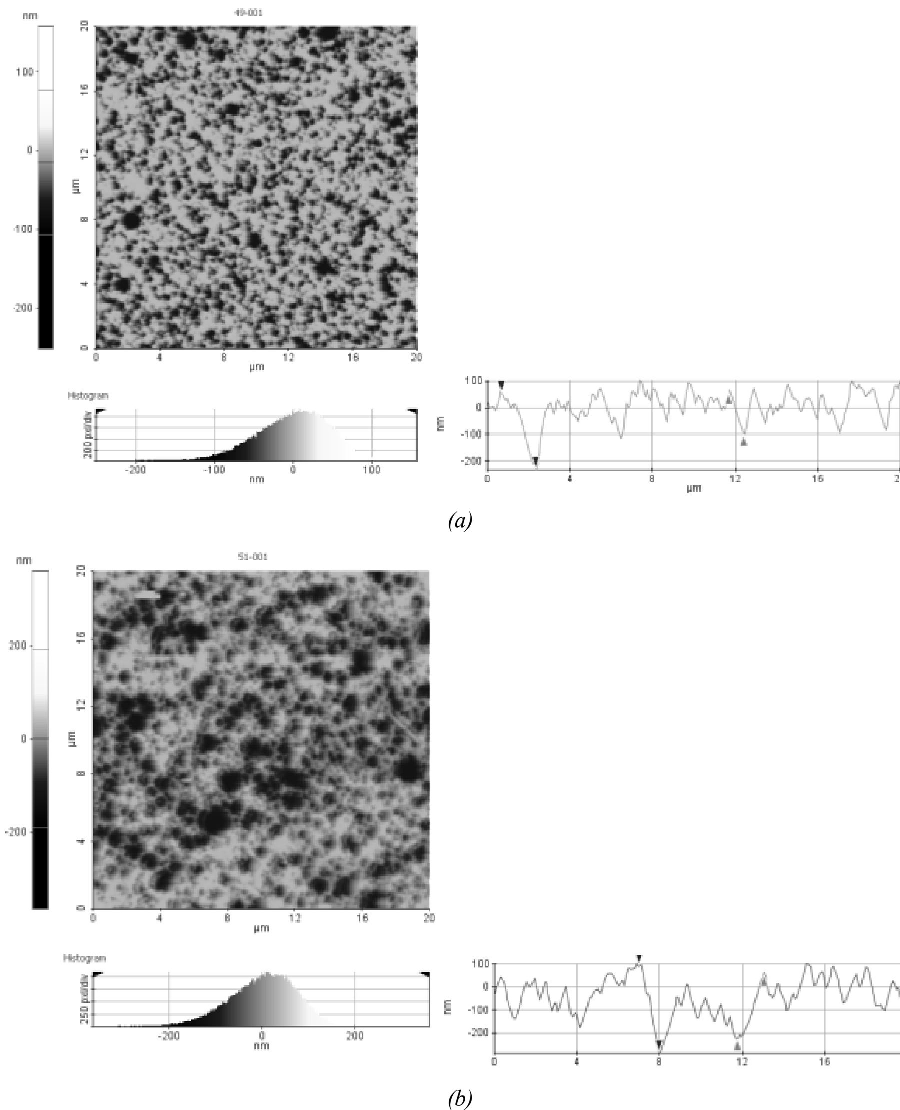

Fig. 3. Depth distribution and cross-section profiles from AFM of GZO films etched for different times. (a) δ_{rms} =46.919 nm, (b) δ_{rms} =72.929 nm.

Etching introduces light scattering and consequently light trapping. The haze factor, which is calculated by the ratio of diffuse to total transmittance, is an indicator for light scattering properties. Depending on the sputtering and etching processes, the haze factors can be tuned over a wide range. Fig. 4 shows high haze factor of 27.16 % at the wavelength of 550 nm is achieved by the GZO film etched for 90 s compared with the value of 16.77 % of commercial SnO_2:F film (Asahi type-U).

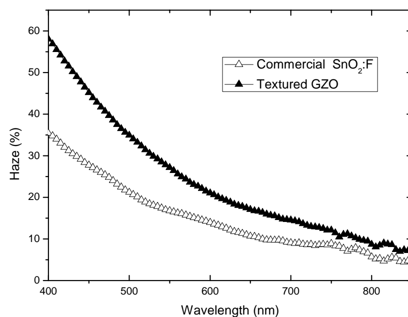

Fig. 4. Haze spectra of textured GZO and commercial SnO_2:F.

3.3 Structure analysis of GZO films etched by various times

The strongest (002) diffraction line at a 2θ value of 34.42° in the X-ray diffraction pattern reveals that the flat GZO films are polycrystalline with hexagonal structure and with c-axis oriented perpendicular to the substrate surface. After etching, the locations of the (002) diffraction peaks do not change significantly. As etching time increases, more films on top are etched, and more films formed initially are exposed. The decease in peak intensity corresponding to the plane (002) as well as the increase in full width at half maximum (FWHM) of the peak indicate the decreased grain size and increased scattering in inter-crystalline boundaries of the films formed initially. In other words, the (002) peak intensity enhances with the increase of thickness, which is consistent with the results of E. Fortunato et al. [13].

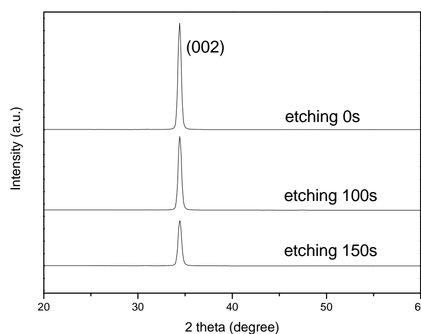

Fig. 5. X-ray diffraction spectra of GZO films etched by different times.

3.4 Application in a-Si:H single junction solar cells

In order to evaluate the quality of textured GZO films, a-Si:H single junction solar cells consisting of glass/ TCO/ (p) a-SiC:H/ (i) a-Si:H

260 nm/ (n) a-Si:H/ GZO/ Al were prepared on optimized textured GZO films, which were obtained from deposition from the target with 3.2 wt.% of Ga_2O_3 and etching in mixed etchant solutions for 90 s. Simultaneously, a reference cell was fabricated on commercial SnO_2:F (Asahi type-U).

The cell based on the doped ZnO coated glass suffers from the ZnO/p contact problem which limits the achievable fill factor [14-16]. The work function difference between n-type ZnO and p-type a-SiC:H causes band bending and builds a potential barrier in the p-layer, which leads to an imperfection ohmic contact. To solve this contact problem, p-type μc-SiC:H [14], n-type μc-Si:H [15] and a-Ge:H [16] were inserted between ZnO and p-type a-SiC:H layer. Here, we utilized a thin (~10 nm) p-type μc-Si:H layer to overcome the high contact resistance. From Table 2, we find an improved fill factor and a slightly decreased current density due to the parasitic absorption loss of the p-type μc-Si:H. There is an increase of 5 % in the cell efficiency with the insertion of p-type μc-Si:H layer. The data also show improved performance of a-Si:H solar cells prepared on optimized textured GZO as compared to on commercial SnO_2:F. The higher values of J_{sc} and efficiency indicate more effective light trapping ability and balanced optical and electrical properties of the optimized textured GZO films. Finally, a short-circuit current density of 14.340 mA/cm^2 and an initial aperture area module efficiency of 8.784 % were obtained on 16×16 cm^2 textured GZO coated glass substrate.

Table 2. Illuminated J-V characteristics of a-Si:H solar cells fabricated on commercial SnO_2:F (#1) with standard p-i-n structure and on textured GZO without (#2) and with (#3) p-type μc-Si:H layer inserted between GZO and p-type a-SiC:H layer.

Cell #	J_{sc} (mA/cm^2)	V_{oc} (V)	FF (%)	Eff. (%)
1	13.955	13.347	68.706	8.530
2	14.520	13.469	64.145	8.363
3	14.340	13.439	68.373	8.784

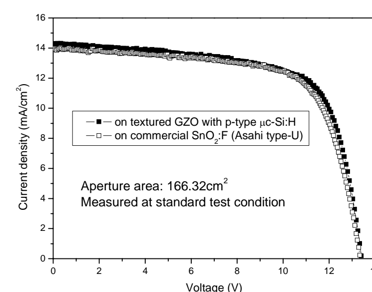

Fig. 6. J-V curves of a-Si:H solar cells prepared on commercial SnO_2:F and on optimized textured GZO.

4. Conclusions

In this study GZO films were deposited at low temperature by rf-magnetron sputtering from ceramic ZnO:Ga_2O_3 targets with different gallium concentrations. As increasing of target gallium concentration, the conductivity of the deposited GZO film increases, but the transmittance in the long wavelength region decreases. The optimum values of figure of merit (F_{TC}) occur at the target gallium concentration of 3.2 and 0.5 wt.% for the wavelength of 400-800 nm and 400-1200 nm, respectively. As for the etching process, a mixture of diluted hydrochloric acid and buffer solutions was used to extend the etching time up to 120 s. The GZO film etched for 90 s has a δ_{rms} value of 72.929 nm and a haze factor of 27.16 % at the wavelength of 550 nm, respectively. X-ray diffraction spectra show that the deposited flat GZO films are polycrystalline with hexagonal structure and with c-axis oriented perpendicular to the substrate surface. As etching time increases, the decease in peak intensity corresponding to the plane (002) as well as the increase in full width at half maximum (FWHM) of the peak indicate the decreased grain size and increased scattering in inter-crystalline boundaries of the films formed initially. Finally, a-Si:H solar cells fabricated on textured GZO show improved performance as compared to on commercial SnO_2:F, confirming the more effective light trapping ability and balanced optical and electrical properties of the optimized textured GZO films.

Acknowledgements

We acknowledge financial support from Electronic Information Industry Foundation of Ministry of Industry and Information Technology of China, Natural Science Foundation of Jiangsu Province (Contract No. BK2008527), Hi-Tech Research Plan of Jiangsu Province (Contract No. BG2007002), Personnel Department of Jiangsu Province (Contract No. 07-E-008) and Science and Technology Commission of Shanghai Municipality (Contract No. 09520714600).

References

[1] J. Löffler, R. E. I. Schropp, Proceedings of the 28th IEEE Photovoltaics Specialists Conference, Anchorage, USA, **892,** (2000).
[2] R. G. Gordon, MRS Bull. **52,** 25 (2000).
[3] E. Fortunato, V. Assunção, A. Marques, I. Ferreira, H. Águas, L. Pereira, R. Martins, Mat. Res. Soc. Symp. Proc. **B5.19.1,** 763 (2003).
[4] T. Nakada, N. Murakami, A. Kunioka, Mat. Res. Soc. Symp. Proc. **411,** 426 (1996).
[5] J. Yoo, J. Lee, S. Kim, K. Yoon, I.J. Park, S.K. Dhungel, B. Karunagaran, D. Mangalaraj, J. Yi, Thin Solid Films **213,** 480 (2005).
[6] M. Berginski, J. Hüpkes, W. Reetz, B. Rech, M. Wuttig, Thin Solid Films **5836,** 516 (2008).
[7] C. Agashe, O. Kluth, J. Hüpkes, U. Zastrow, B. Rech, J. Appl. Phys. **1911,** 95 (2004).
[8] E. Burstein, Phys. Rev. **632,** 93 (1954).
[9] T. S. Moss, Proc. Phys. Soc. B **775,** 67 (1954).
[10] G. Haacke, J. Appl. Phys. **4086,** 47 (1976).
[11] J. Müller, G. Schöpe, O. Kluth, B. Rech, M. Ruske, J. Trube, B. Szyszka, X. Jiang, G. Bräuer, Thin Solid Films **327,** 392 (2001).
[12] O. Kluth, B. Rech, L. Houben, S. Wieder, G. Schöpe, C. Beneking, H. Wagner, A. Löffl, H.W. Schock, Thin Solid Films **247,** 351 (1999).
[13] E. Fortunato, L. Raniero, L. Silva, A. Gonçalves, A. Pimentel, P. Barquinha, H. Águas, L. Pereira, G. Gonçalves, I. Ferreira, E. Elangovan, R. Martins, Sol. Energy Mater. Sol. Cells **1605,** 92 (2008).
[14] W. Ma, S. Aoyama, H. Okamoto, Y. Hamakawa, Sol. Energy Mater. Sol. Cells **453,** 41 (1996).
[15] M. Kubon, E. Böhmer, F. Siebke, B. Rech, C. Beneking, H. Wagner, Solar Energy Mater. Solar Cells **485,** 41 (1996).
[16] G. Ganguly, D.E. Carlson, S.S. Hegedus, D. Ryan, R.G. Goldon, D. Pang, R.C. Reedy, Appl. Phys. Lett. **479,** 85 (2004).

* Corresponding author: guohua_li55@yahoo.com